Cellulose (2018) 25:5739–5750
https://doi.org/10.1007/s10570-018-1977-y

ORIGINAL PAPER

A multistep mild process for preparation of nanocellulose from orange bagasse

Mayra A. Mariño · Camila A. Rezende · Ljubica Tasic

Received: 31 January 2018 / Accepted: 4 August 2018 / Published online: 7 August 2018

Abstract Orange bagasse *in natura* and industrial orange bagasse were investigated as starting materials for the production of nanocellulose under moderate chemical sequential extraction conditions. The latter accounted for acid (5% v v^{-1} and 100 °C) and/or alkaline conditions (NaOH 1.6–4.0% m v^{-1}, 120 °C); and bleaching with $NaClO_2$ (1–3% m v^{-1}, 80 °C). Ultrasound treatment yielded very similar cellulose nanofibers with 60–70% of crystallinity and highly pure (over 98%). As seen by field emission scanning electron microscopy, cellulose nanofibers showed mean diameters of 18.4 nm ± 6.0 nm from bagasse *in natura*, while 20.5 nm ± 7.0 nm mean diameters were observed for the nanofibers isolated from the industrial bagasse. Crystallinity indices were determined using X-ray diffraction and solid-state nuclear magnetic resonance (CP–MAS ^{13}C NMR) data. The obtained materials have numerous potential applications and represent a green alternative for the treatment of orange fruit biomass.

M. A. Mariño · L. Tasic (✉)
Department of Organic Chemistry, Institute of Chemistry, University of Campinas, P.O. Box 6154, Campinas, SP 13083-970, Brazil
e-mail: ljubica@iqm.unicamp.br

C. A. Rezende
Department of Physical Chemistry, Institute of Chemistry, University of Campinas, Campinas, SP, Brazil

Graphical abstract

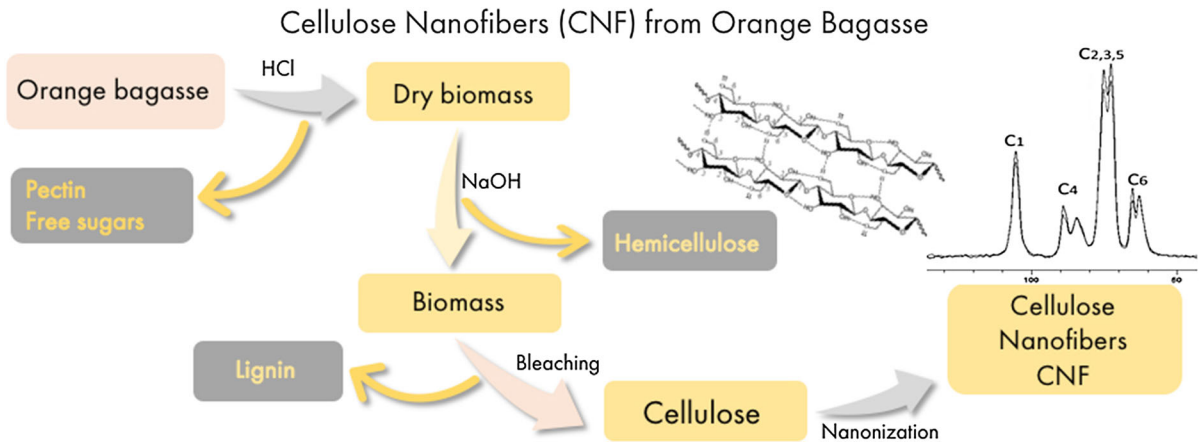

Keywords Orange bagasse · Cellulose nanofibers (CNFs) · Chemical sequential extraction · Green chemistry

Introduction

Orange bagasse (OB) is a global agroindustry by-product from the juice processing companies and a common type of biomass generated even in our day-to-day routine. Brazil, China, United States, European Union (Mediterranean countries), and Mexico (USDA 2017) are the leading countries in orange production. This common biomass presents low lignin (3–5%, on a dry basis) and high pectin contents (up to 25%, on a dry basis), besides hemicellulose and cellulose (up to 20%, on a dry basis) in its composition. After juice extraction or processing, the biomass contains peel, seeds and pulp, and the industrial one is subjected to filtering, pressing and drying, which result in a compact residue (citrus pulp-pellets, CPPs) used as supplement for animal feed.

Research on exploitation of orange bagasse (OB) has been dedicated to sugar recovery, fermentation, polysaccharide recovery (pectin), essential oils or/and flavonoids extractions (Rezzadori et al. 2012). Among OB fermentation products, metabolites such as ethanol (Nigam and Pandey 2009), citric acid (Rivas et al. 2008), L-lactic acid (Ge et al. 2014) and succinic acid (Li et al. 2010) are highlighted. OB has also been investigated as a substrate for production of pectinases (Nigam and Pandey 2009; Ahmed and Mostafa 2013) and xanthans (Bilanovic et al. 1994). After a mild chemical sequential extraction of lignocellulosic components, solid residues usually contain cellulose and lignin remnants. These residues could be burned for heat, electricity generation (Nigam and Pandey 2009) or could be a source of cellulose, which has multiple applications (Kalia et al. 2011). However, for the former purpose, the high moisture content of OB (up to 80%) is an important impediment to energy generation. For the latter purpose, the hydrolysis of cellulose is usually performed at high acid concentration to remove the amorphous cellulose fractions and obtain cellulose nanocrystals (CNCs) or cellulose nanofibers (CNFs). The strong acid treatment depolymerizes the cellulose and the CNCs have a needle-like morphology and narrow size distribution (Habibi et al. 2010) while CNFs with a high degree of polymerization are produced in several ways, including less-strong acid, alkaline solution, enzymatic hydrolysis, or mechanical grinding (Mariño et al. 2015; Mittal et al. 2011). However, the enzymatic hydrolysis involves high production cost because it requires the use of purification techniques for enzymes' concentration (Campos et al. 2013). Therefore, mild chemical treatments (Duchemin 2015) might be considered as cheaper options for CNF production. Dry orange peel suffers saccharification when treated with sulfuric acid and an increase in cellulose crystallinity, while alkaline treatment (low concentrations of NaOH) can be used for cellulose recovery (Bicu and Mustata 2013). These nanocellulose materials—cellulose

nanofibers (CNFs) and cellulose nanocrystals (CNCs)—might have many interesting applications among which we can cite their potential use in water purification (Voisin et al. 2017), drug delivery (Rao et al. 2017), tissue engineering (Kumar et al. 2014), composite preparations (Habibi et al. 2010) and others.

Our research is focused on a sequential extraction of orange bagasse for CNF preparation. Two types of biomasses were investigated: (1) a biomass obtained after juice squeezing, which was named orange bagasse *in natura* (OBN), and (2) a biomass of the citrus pulp-pellets (CPPs) that were obtained after pressing the OBN treated with the calcium oxide before being pelletized and dried, which was named industrial orange bagasse (IOB). The biomasses processing started with a NaOH treatment at mild pressure, combined with an acid or a base extraction and a high-pressure defibrillation (ultrasonication). Particular emphasis was given on the characterization of CNFs obtained at different physical–chemical conditions.

Experimental section

Materials

Cellulose nanofibers were extracted from two different sources of OB. The first source was an orange waste from the production of orange juice (bagasse *in natura*) obtained after squeezing the oranges. The second one was the citrus pulp pellet biomass, which was obtained after OB pressing, drying and pelletizing. These residues were obtained from a Brazilian orange-juice processing industry (Citrosuco, Matão, São Paulo, Brazil). Both biomasses correspond to the same species (*Citrus sinensis* (L) *osbeck,* variety). OBN and IOB were cut into small pieces (1–3 cm) and OBN was oven-dried at 100 °C. Dry bagasse was ground and sieved to a fraction with particle sizes smaller than 1 mm. The ground bagasse was further boiled with a hydrochloric acid solution at pH 2.00 (ratio 1:30 biomass/solution, w v^{-1}) and filtered until the fibers were pectin-free and sugar-free. The resulting fibers were once again oven-dried at 100 °C and used for CNF extraction.

Methods

Extraction of cellulose and preparation of cellulose nanofibers

OB was treated with NaOH 1.6%, 2%, 3% and 4% (w v^{-1}) solutions, at 120 °C under an autoclave pressure (around 1 atm) for 20 min to remove hemicelluloses. Afterward, the bleaching process of the insoluble residue was carried out at 80 °C, pH 4.5 for 30 min. For OBN this step was successful when sodium chlorite 1% m v^{-1} (1:10 fibers to volume mass ratio) was used. However, the bleaching treatment for IOB was performed with a concentration 3.0% m v^{-1} of sodium chlorite and an additional step using 6.5% v v^{-1} of H_2O_2 at pH 10.0 and 80 °C for 30 min. All residual reagents were removed by filtration with hot water.

The treated material underwent an additional extraction step using: (a) sulfuric acid (5–10% v v^{-1}) or (b) NaOH solution under the aforementioned conditions. The conditions for the acid step were boiling solution for 30 min and ratio 1:8 w v^{-1} (biomass residue: acid solution) and dialysis against deionized water after washing and filtration (3.5 kDa cut-off, Fisher *Sci*).

An aqueous suspension of the obtained cellulose fibers was sonicated for 5 min (Misonix, Ultrasonic Liquid Processors with a tip). The homogenization process by sonication was performed three times for OBN.

Characterization methods

Compositional analysis on dry matter basis

The hemicellulose and the cellulose extractions from raw materials were evaluated according to the protocols of ANKOM technology (USA) after removal of pectin and water-soluble fractions. The difference between acid detergent fiber (ADF) and acid detergent lignin (ADL) filter bag techniques were reported as cellulose content (AOAC 2000). The pectin extraction and quantification were carried out using the method of Sudhakar and Maini (2000). The water-soluble fraction was extracted using deionized water at 80 °C.

Fourier transform infrared (FTIR) spectroscopy

The chemical structures of the nanocellulose samples were studied by FTIR ATR spectroscopy using oven-dried samples (CARY 630 Spectrophotometer-Agilent Technologies, USA). Each spectrum was obtained by accumulating 128 scans at a resolution of 4 cm^{-1} in the 4000–400 cm^{-1}.

XRD analysis

Lyophilized nanocellulose samples were analyzed using XRD. A Shimadzu XRD-7000 X-ray diffractometer (USA) operating at 40 kV and 30 mA was used to obtain the diffraction profile at 2° per min, and data were recorded using a copper (Kα) radiation source. Diffraction patterns were scanned over a 2θ range of 5.00°–50.00°, and the CI were calculated using the following equation, according to Segal empirical formula (1962):

$$CI = \frac{I - Ia}{I} \quad (1)$$

where I is the total intensity value at 22.7° 2θ and Ia is the minimum intensity value at 18° 2θ depicted in figures as I_{AM} that accounts for intensity of the amorphous cellulose (Nam et al. 2016; Park et al. 2010; Peng et al. 2013; Terinte et al. 2011).

NMR spectroscopy analysis

A Bruker AMX-300 MHz instrument, operating at 7.05 T, with cross-polarization and magic angle spinning (CP/MAS) was used for recording the ^{13}C NMR spectra at 75.47 MHz. We have used a 90° pulse for 1.5 ms and an 800-ms contact pulse sequence at 3000 Hz MAS rate. Spectra were recorded with 10,000 scans and 3.0 s delays between each repetition.

Multiple peak fitting was done using the deconvolution method and assuming a Gaussian line shape for the cellulose C-4 peaks to determine the CI. The C-4 peak area from 86 to 92 ppm was assigned to crystalline cellulose and the total area comprised the region from 79 to 92 ppm (Vanderhart and Atalla 1984).

Morphological analysis

The morphological characteristics of CNFs were investigated using a Quanta field emission scanning electron microscope (FESEM-FEI 250 Quanta™) and transmission electronic microscope (TEM, Libra 120, Carl-Zeiss). The sonicated nanocellulose dispersion was dropped onto a sample holder, covered with porous carbon film, dried at room temperature and coated with a gold layer of 3–4 nm using a MED 020 Sputter (BalTech). Images were obtained using a 10 kV accelerating voltage and a secondary electron detector during FESEM analyses. For TEM a drop of a diluted suspension of nanocellulose was deposited on carbon-coated grids and let dry at room temperature. The fiber mean diameters were measured in TEM and FESEM images using the ImageJ 1.50 software (National Institute of Health-NIH, USA). For this purpose, 20 segments were randomly selected.

Samples were also analyzed by scanning probe microscopy (SPM, Shimadzu WET-SPM) in the non-contact and phase modes. The suspensions prepared from the products of OBN and IOB were air-dried at 40 °C and the resulting film was then analyzed at room temperature.

Commercial Si nanoprobe tips (NCHR-20, Nano World) with a resonance frequency of 320 kHz and force constant of 42 N m^{-1} were used to scan the samples. At least three different regions for each sample were scanned and twenty images per sample were analyzed.

Results and discussion

Chemical composition

The results of the chemical composition for the comparative analysis between OBN and IOB are shown in Table 1. OBN was considered as a biomass more

Table 1 Chemical composition of orange bagasse (OBN) *in natura* and industrial orange bagasse (IOB)

Source	OBN	IOB
Water-soluble fraction (%)	48.11 ± 2.11	42.04 ± 4.78
Pectin (%)	24.46 ± 5.38	27.16 ± 1.39
Cellulose (%)	11.85 ± 2.73	21.04 ± 7.43
Hemicellulose (%)	15.58 ± 2.07	9.75 ± 1.07
Lignin (%)	1.67 ± 0.88	3.50 ± 0.09

amenable to fermentation due to its higher water-soluble fraction. However, IOB has higher cellulose and lower hemicellulose contents. Results for OBN were consistent with the ones reported in the literature (Rezzadori et al. 2012; Oberoi et al. 2010; Bicu and Mustata 2013), in which cellulose contents laid within 10–15%, hemicelluloses contents within 10–13% and lignin contents in the 0.6–1.0% range. While higher cellulose and lignin contents of IOB might be associated with the presence of leaves and branches in the biomass.

FTIR spectroscopy of cellulosic materials

Figure 1 shows FTIR ATR spectra of CNFs obtained after a sequential extraction of OBN and IOB.

The FTIR data of CNFs from OBN or IOB are similar. The most important cellulose bands correspond to intermolecular hydrogen bonding between the hydroxyl groups on C-2 and C-6 of the pyranose ring at 3330 cm^{-1}, C–H and C–O–C motions of the pyranose ring at 2870–2920 cm^{-1} and 1160–1030 cm^{-1}, respectively. Minor bands correspond to the $–CH_2–$ symmetric and wagging bending of C-6 that were observed between 1380 and 1310 cm^{-1}, while the characteristic band for the β-glycosidic linkages between glucose units was observed at 900 cm^{-1} (Alemdar and Sain 2008; Cherian et al. 2008).

Spectral bands that reflect the presence of other remaining components were observed in the 1400–1750 cm^{-1} region. It was possible to elucidate the presence of lignin; hemicelluloses or pectin by the stretching vibration of C-O bond for esters at 1730 cm^{-1}, although the presence of the latter should be discarded due to the acidic pre-treatment. A more specific characteristic for lignin is the stretching vibration of aromatic rings, at 1440–1600 cm^{-1}, which was considered as a fraction of insoluble lignin. However, these peaks are present in low intensity, which supports the idea of detaching mainly cellulosic products from both samples.

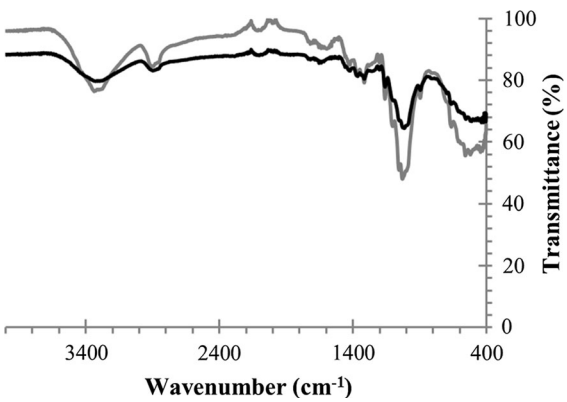

Fig. 1 FTIR attenuated total reflectance (ATR) spectra of CNFs obtained after sequential extraction of orange bagasse *in natura* (OBN, black) and industrial orange bagasse (IOB, gray)

A variation observed in these spectra was a sharper peak at 3330 cm^{-1} of the product from IOB, which is related to a more intense disruption of the hydrogen bonds at the C-3 and C-6 positions in the cellulose. Therefore, a higher capacity to absorb water is expected for this source material due to a higher NaOH concentration used during its sequential extraction (Cherian et al. 2008; Abraham et al. 2011).

Cellulose extraction analyzed by XRD

Figures 2 and 3 show the XRD patterns obtained for the best CNF products obtained from OBN and IOB, respectively. Peaks $1\bar{1}0$, 110, 200 (22.7° 2θ), 004 (35° 2θ) were depicted. Peak broadening and overlap was probably caused by reduction in crystallinity of CNFs (Thygesen et al. 2005) when compared to cellulose nanocrystals (CNCs).

Tables 2 and 3 show CI values for CNFs from OBN and IOB, respectively. Two of the CNF samples from each OB were also analyzed by CP-NMR ^{13}C NMR.

The higher lignin content in IOB, which might act as an adhesive agent, was a probable cause of poorer results in extracting cellulose nanofibers from this biomass (French 2014), as indicated by the lower CI for CNFs when 2% NaOH was used. Nevertheless, α-aryl ether linkages between hydroxyl lignin groups and hydroxyl groups from polysaccharides (hemicelluloses and cellulose), as well as ester bonds from the uronic acid (hemicelluloses) with lignin hydroxyl groups (Peng et al. 2012; Cherian et al. 2011) were disrupted during the 2% alkaline treatment repeated twice.

The CI values for CNFs obtained herein were similar to some published data. For instance, banana cellulose nanofibers obtained with a 2% NaOH solution and treated with 5% and 11% of oxalic acid solution resulted in fibers with 68% and 74% of crystallinity, respectively. Pineapple leaves were treated with the same process using solution of oxalic acid (11%) after mercerization in a 2% NaOH solution, and the cellulose fibers obtained had a CI

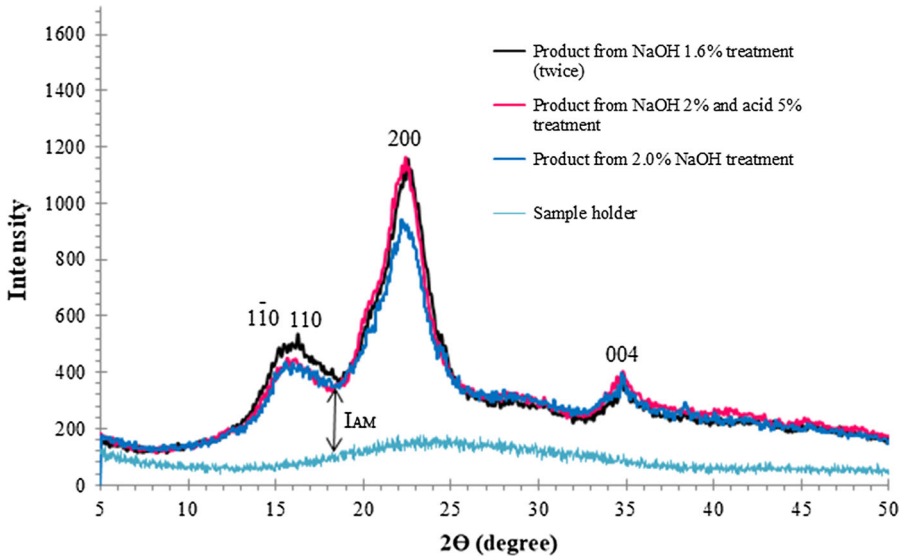

Fig. 2 XRD patterns for CNFs resulting from sequential extraction of orange bagasse *in natura* (OBN)

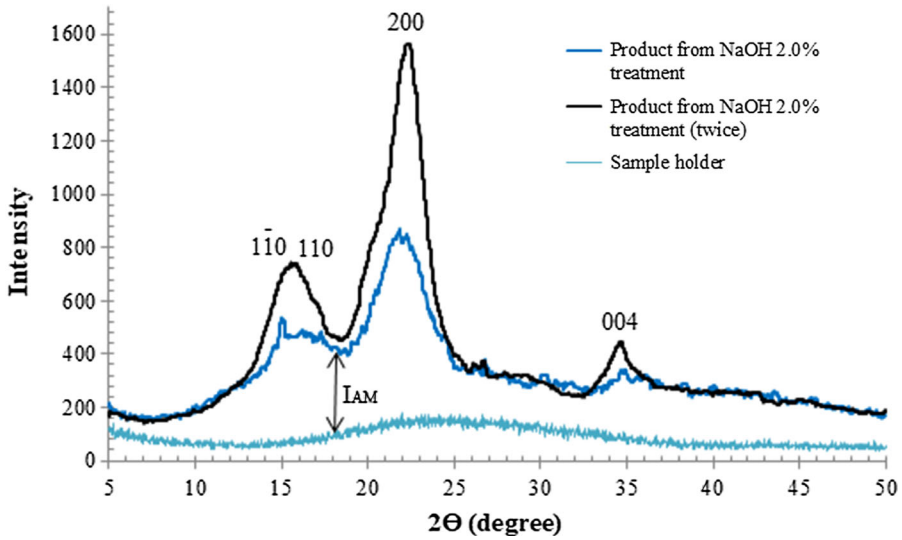

Fig. 3 XRD patterns for CNFs resulting from sequential extraction of industrial orange bagasse (IOB)

Table 2 Crystallinity indices (CI) for cellulose nanofibers obtained from OBN after sequential extraction and bleaching with $NaClO_2$ (1% m v^{-1})

Sample	CI by XRD	CI by NMR
CNF-NaOH (1.6%)	0.70	–
CNF-NaOH (2.0%)	0.71	–
CNF-NaOH (3.0%)	0.71	–
CNF-NaOH (2.0%) and H_2SO_4 (5.0%)	0.79	0.58
CNF-NaOH (1.6%) twice	0.73	0.52

Table 3 Crystallinity indices for nanocellulose fibers obtained from the IOB in sequential extraction and two-steps bleaching using $NaClO_2$ (3% m v^{-1}) and H_2O_2 (6.5% v v^{-1})

Sample	CI by XRD	CI by NMR
CNF-NaOH (2.0%)	0.55	–
CNF-NaOH (3.0%)	0.72	–
CNF-NaOH (1.6%) (4.0%)	0.72	–
CNF-NaOH (3.0%) and H_2SO_4 (5.0%)	0.72	–
CNF-NaOH (3.0%) and H_2SO_4 (10%)	0.77	0.60
CNF-NaOH (2.0%) twice	0.77	0.58

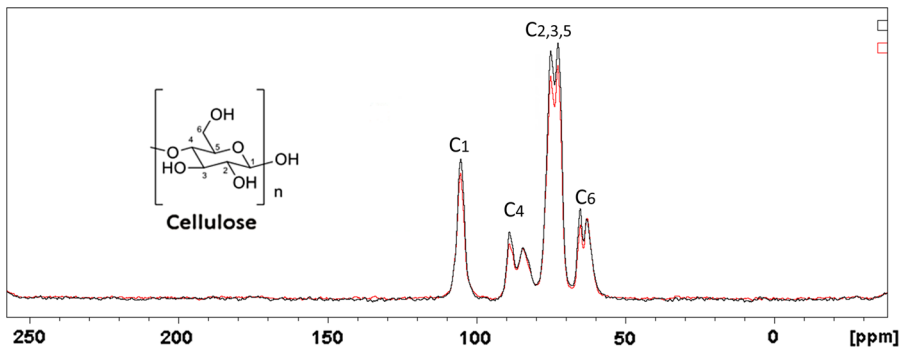

Fig. 4 CP/MAS ^{13}C NMR spectra of cellulose nanofibers (CNFs) obtained from OBN (red) and IOB (black) after NaOH sequential extraction (two-step process before the bleaching process). Cellulose structure and C-atoms numbering are given in upper left corner. (Color figure online)

around 74%. In other report, wheat straw and soy hulls were treated with a 1 mol L^{-1} HCl solution after mercerization with NaOH 17.5% and resulted in products with 78% and 70% crystallinity, respectively. Considering these values, it is easy to notice a significant difference regarding the NaOH concentration used in the aforementioned studies (Abraham et al. 2011).

High NaOH concentrations are generally used for biomasses with high lignin levels or for alkaline treatment at atmospheric pressure. Therefore, it is essential to determine the adequate NaOH load (liquid-to-solid ratio) and choose the best condition for the process of extracting the CNFs from each biomass (Bicu and Mustata 2013). Few studies (Bicu and Mustata 2013; Zuluaga et al. 2009) have reported on the influence of the NaOH load for non-cellulosic components removal from a specific biomass. Nevertheless, at high-pressure conditions, it is better to use a low NaOH concentration to avoid cellulose degradation (Cherian et al. 2011).

In this study, a two-step alkaline sequential extraction with low NaOH load (1.6 or 2%) against OB was the best option for producing the cellulose nanofibers with the high CI (70%). In quantitative terms, the yield of the nanocellulose from IOB (18.40%) was higher than from OBN (10.78%), and these were values close to the cellulose contents in the respective raw materials (21.00% and 11.90%, respectively).

CP/MAS ^{13}C NMR data

CP/MAS ^{13}C NMR spectra of freeze-dried CNFs after two-step sequential extraction with NaOH and bleaching are shown in Fig. 4 and reveal only variations in the peak intensities characteristic for cellulose. Peaks C-2, C-3 and C-5 are overlapping (72–76 ppm) and peaks C-6 and C-4 correspond to crystalline and amorphous fractions of cellulose.

The ratio of areas at the C-4 crystalline fraction of cellulose and total line-fit area gave the following CI values: 0.60 for CNFs from OBN treated with 1.6% NaOH solution (twice) and 0.60 for CNFs from IOB treated with 2.0% NaOH solution (twice). These values are somewhat lower in comparison to the ones obtained with XDR (70%). Just a few studies used CP/MAS ^{13}C NMR for quantitative characterization of cellulosic materials (Zhao et al. 2006; Hult et al. 2002; Chimentão et al. 2014; Mariño et al. 2015). CI values

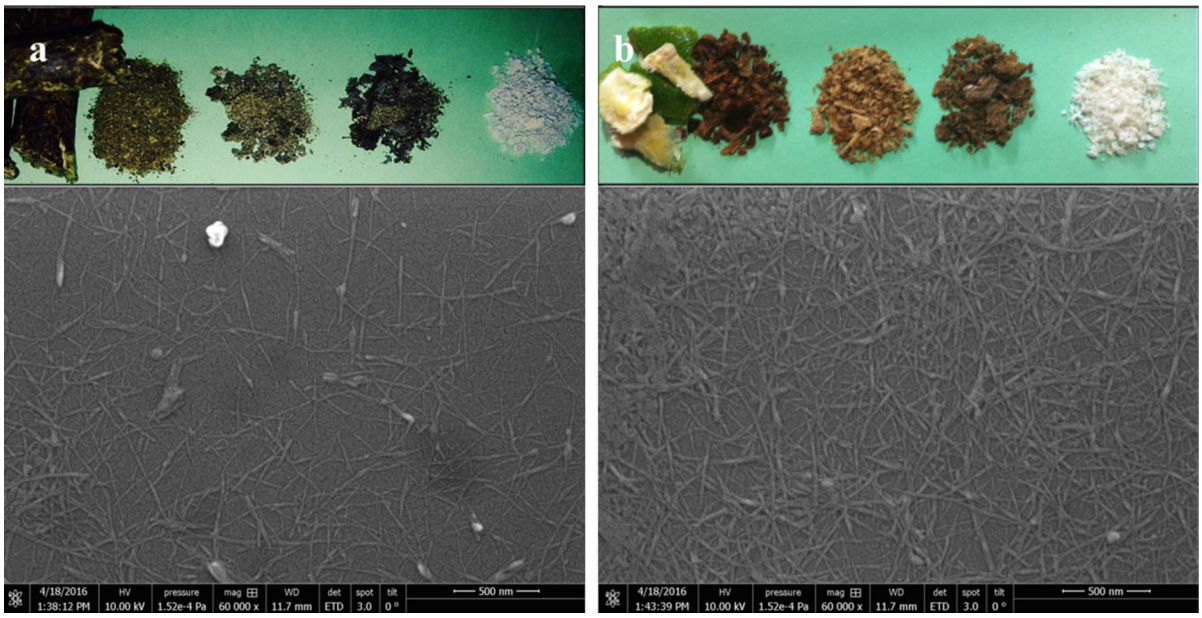

Fig. 5 Upper panels: photographs of orange bagasse from the beginning to the end of processing into cellulose nanofibers (CNFs). From left to right are shown: raw materials, raw materials after milling and oven-drying, fiber residues after pectin removal, NaOH-treated fibers and final products after bleaching processes for: **a** IOB and **b** OBN. Lower panels: FESEM micrographs showing the CNFs

obtained from earlier reports using acid-diluted hydrolysis of microcellulose (Zhao et al. 2006; Hult et al. 2002) were similar to the obtained in this research. However, a higher crystallinity (70%) was obtained by Chimentão et al. (2014) by hydrolysis with a 3% wt oxalic acid solution. It's worth noting that the crystallinity gain was slight in both studies (around 3–4%); while the hydrolysis with H_2SO_4 had a particular effect on the cellulose, once its crystallinity suffered a decrease with a 6% solution and an increase with a 3% solution at 120 °C. OBN hydrolysis with enzymes from *Xanthomonas axonopodis* pv. *citri* (Mariño et al. 2015), reported on lower CNF crystallinity.

Morphology of nanocellulose fibers

The nanostructure and size of the CNFs homogenized by ultrasonication were investigated by FESEM and by SPM after sonication and air-drying. The micrographs in Figs. 5 and 6 show that the nanofibers of interest were obtained from the micrometer-length hydrolyzed material after the mechanical treatment applied. The mean diameter and length of the fibers

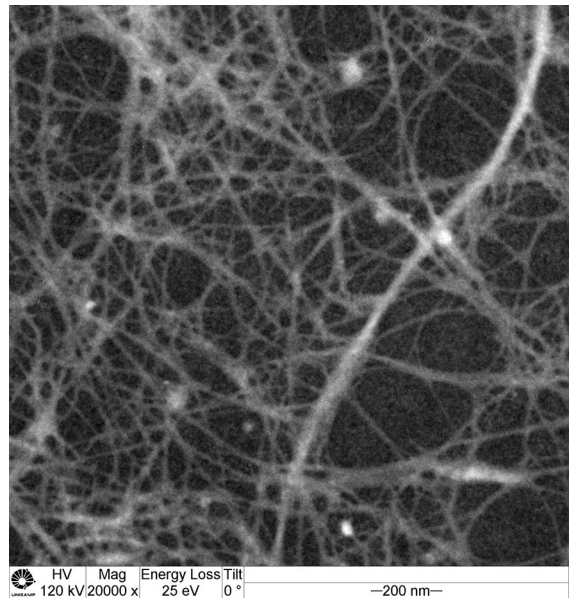

Fig. 6 Morphology of the sonicated CNFs from IOB represented by transmission electron micrograph (TEM)

were calculated by an image processing software (ImageJ 1.49°).

Both CNF samples showed a narrow diameter distribution. The fiber diameters obtained from the

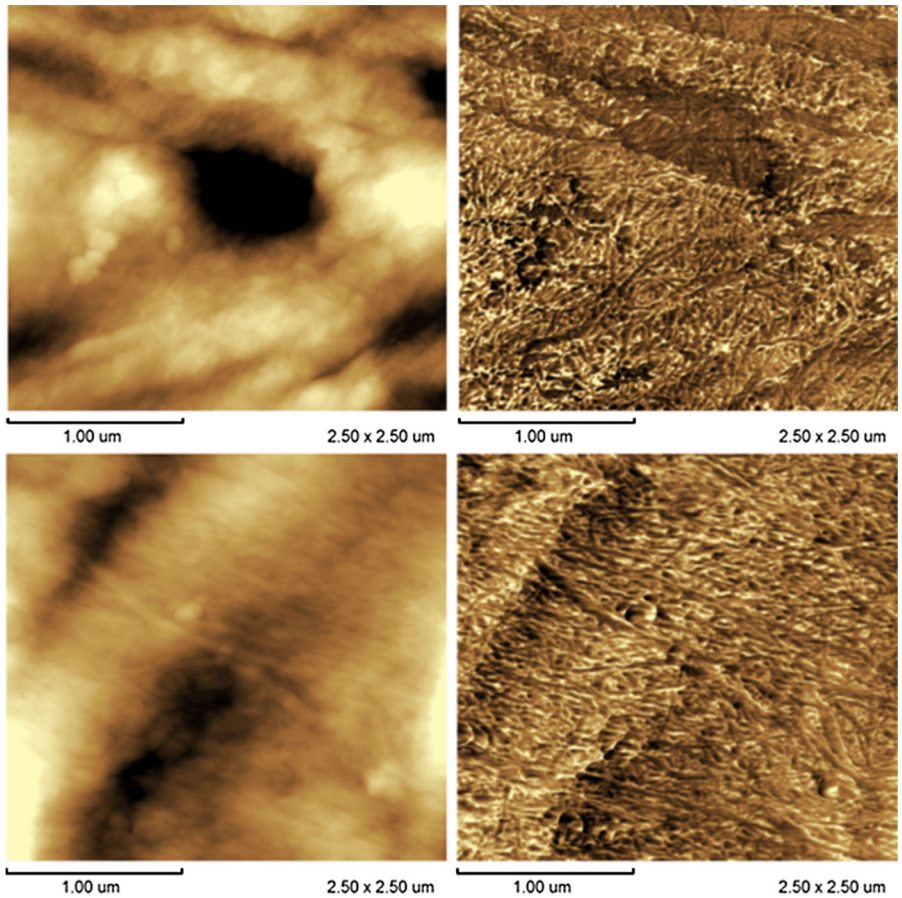

Fig. 7 Scanning probe micrographs of nanofibers in a film prepared by air-drying of the cellulosic material obtained from OBN: topography on the left and phase images on the right

OBN, were 18.40 nm ± 5.88 nm; and, from IOB mean diameters were 20.50 nm ± 7.20 nm.

The fiber aspect ratio (fibril length to diameter ratio) was difficult to be calculated, due to the web-like network distribution of the microstructure, where there is an invisible portion of the fiber total length, which is usually covered by other fibers. Presumably, the other samples possess a similar aspect ratio and this result is in accordance with CNFs produced in an earlier study (Mariño et al. 2015).

A large aspect ratio is related to an enhanced reinforcement capacity compared to cellulose nanocrystals. In spite of that, a nanofibril with large length obtained by mild or moderate hydrolysis involves a reduced crystallinity. Both cellulose nanofibers and cellulose nanocrystals acting as reinforcement nanofillers improve the mechanical properties of polymeric matrices (Xu et al. 2013).

When air-dried from concentrated suspensions, cellulose nanofibers form a film that was imaged by SFM. Figures 7 and 8 show topography images on the left and phase images on the right, obtained in OBN and IOB samples, respectively. Fiber relief is very clear in phase images, showing their packed arrange in the film.

Conclusions

Citrus cultivation is one of the most important agricultural activities in Brazil and is usually characterized by two or three flowering seasons per year (March-December). After harvest, a by-product—orange bagasse (OB)—is obtained as ½ of all fruit. It contains free sugars, such as fructose and glucose (16–25%), lignin, pectin, hemicelluloses, cellulose

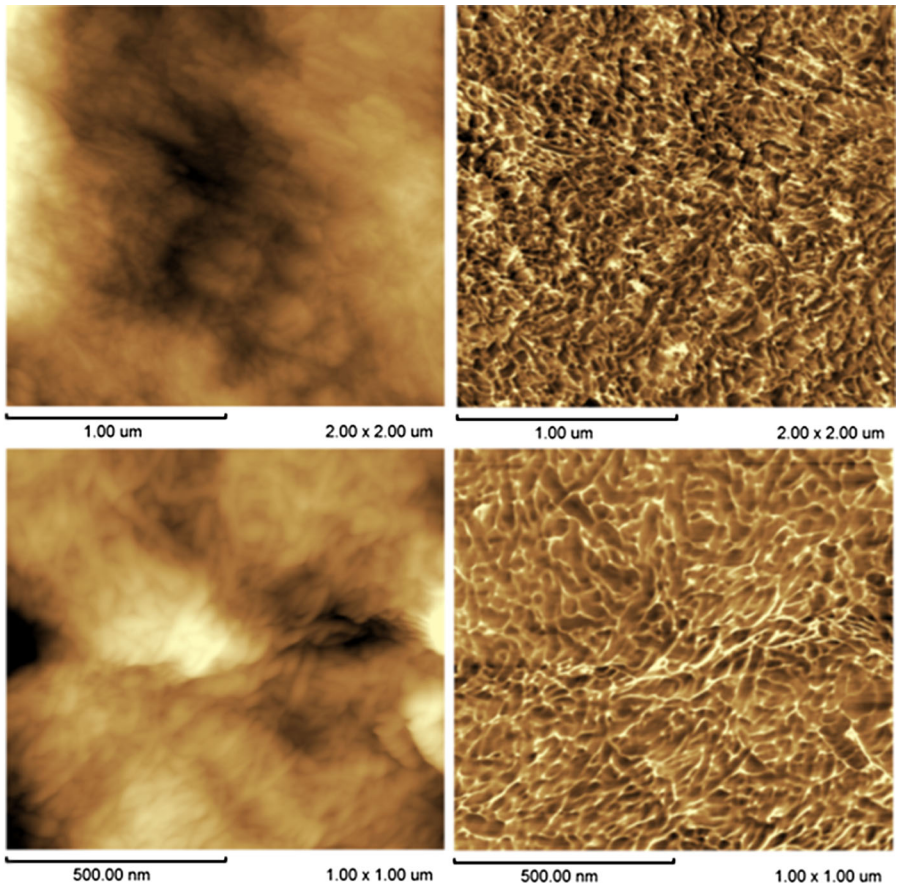

Fig. 8 Scanning probe micrographs of nanofibers in a film prepared by air-drying of the cellulosic material obtained from IOB: topography on the left and phase images on the right

and might be valued for bioethanol production and cellulose extraction. Two orange bagasse sources were exploited for cellulose recovery, orange bagasse *in natura* (OBN) and industrial orange bagasse (IOB). Chemical sequential extraction was conducted in mild conditions with diluted acid or alkaline solutions. A two-step alkaline (2% NaOH) sequential extraction was shown to be the most successful for cellulose nanofibers (CNFs) production with high yields of 10.78% (OBN) and 18.4% (IOB). The OBN was more susceptible to sequential extraction, but the IOB presented higher yield and needed lower energy consumption for the preparation of cellulose nanofibers. Both OB cellulose nanofibers showed crystallinity of around 60–70%, and mean diameters of around 20 nm. The obtained CNFs have numerous potential applications and might add value to this common agroindustry waste that pollutes our environment.

Acknowledgments The authors thank funding agencies: *Coordenação de Aperfeiçoamento de Pessoal de Ensino Superior* (CAPES), *Conselho Nacional de Pesquisa* (CNPq) and *Fundação de Amparo à Pesquisa do Estado de São Paulo* (FAPESP).

Compliance with ethical standards

Conflict of interest The authors declare that they have no conflict of interest.

References

Abraham E, Deepa BL, Pothan A, Jacob M, Thomas S, Cvelbar U, Anandjiwala R (2011) Extraction of nanocellulose

fibrils from lignocellulose fibres: a novel approach. Carbohydr Polym 86:1468–1475
Ahmed SA, Mostafa FA (2013) Utilization of orange bagasse and molokhia stalk for production of pectinase enzyme. Braz J Chem Eng 30:449–456
Alemdar A, Sain M (2008) Isolation and characterization of nanofibers from agricultural residues—wheat straw and soy hulls. Bioresour Technol 99:1664–1671
AOAC. Official Methods of Analysis (2000) Association of official analytical chemists, vol 2, 17th edn. AOAC International, Gaithersburg
Bicu I, Mustata F (2013) Optimization of isolation of cellulose from orange peel using sodium hydroxide and chelating agents. Carbohydr Polym 98:341–348
Bilanovic D, Shelef G, Green M (1994) Xanthan fermentation of citrus waste. Bioresour Technol 48:169–172
Campos A, Correa AC, Cannella D, Teixeira EM, Marconcini JM, Dufresne A, Mattoso LC, Cassland P, Sanadi AR (2013) Obtaining nanofibers from curauá and sugarcane bagasse fibers using enzymatic hydrolysis followed by sonication. Cellulose 20:1491–1500
Cherian BM, Pothan LA, Nguyen-Chung T, Mennig G, Kottaisamy M, Thomas S (2008) A novel method for the synthesis of cellulose nanofibril whiskers from banana fiber and characterization. J Agric Food Chem 56:5617–5627
Cherian BM, Leão AL, Souza SF, Thomas S, Pothan LA, Kottaisamy M (2011) Isolation of nanocellulose from pineapple leaf fibres by steam explosion. Carbohydr Polym 81:720–725
Chimentão RJ, Lorente E, Gispert-Guirado F, Medina F, López F (2014) Hydrolysis of dilute acid-pretreated cellulose under mild hydrothermal conditions. Carbohydr Polym 111:116–124
Duchemin BJC (2015) Mercerization of cellulose in aqueous NaOH at low concentrations. Green Chem 17:3941–3947
French AD (2014) Idealized powder diffraction patterns for cellulose polymorphs. Cellulose 21:885–896
Ge X, Xu Y, Chen X, Zhang L (2014) Improvement of l-lactic acid production from orange peels in mixed culture system. J Glob Biosci 3:354–360
Habibi Y, Lucia AL, Rojas OJ (2010) Cellulose nanocrystals: chemistry, self-assembly, and applications. Chem Rev 110:3479–3500
Hult E, Liitiä T, Maunu SL, Hortling B, Iversen TA (2002) CP/MAS ^{13}C-NMR study of cellulose structure on the surface of refined kraft pulp fibers. Carbohydr Polym 49:231–234
Kalia S, Dufresne A, Cherian BM, Kaith BS, Avérous L, Njuguna J, Nassiopoulos E (2011) Cellulose-based bio- and nanocomposites: a review. Int J Polym Sci. https://doi.org/10.1155/2011/837875
Kumar A, Negi YS, Choudhary V, Bhardwaj NK (2014) Microstructural and mechanical properties of porous biocomposite scaffolds based on polyvinyl alcohol, nano-hydroxyapatite and cellulose nanocrystals. Cellulose 21:3409–3426
Li Q, Siles JA, Thompson IP (2010) Succinic acid production from orange peel and wheat straw by batch fermentation of *Fibrobacter succinogenes* S85. Appl Microbiol Biotechnol 88:671–678
Mariño M, Lopes L, Durán N, Tasic L (2015) Enhanced materials from nature: nanocellulose from citrus waste. Molecules 20:5908–5923
Mittal A, Katahira R, Himmel M, Johnson D (2011) Effects of alkaline or liquid-ammonia treatment on crystalline cellulose: changes in crystalline structure and effects on enzymatic digestibility. Biotechnol Biofuels 4:41–56
Nam S, French AD, Condon BD, Concha M (2016) Segal crystallinity index revisited by the simulation of X-ray diffraction patterns of cotton cellulose Iβ and cellulose II. Carbohydr Polym 135:1–9
Nigam PS, Pandey A (2009) Production of organic acids from agro-industrial residues. In: Singh P, Pandey A (eds) Biotechnology for agro-industrial residues utilisation—utilization of agro-residues. Springer, Basingstoke, pp 37–60
Oberoi HS, Vadlani PV, Madl RL, Saida L, Abeykoon JP (2010) Ethanol production from orange peels: two-stages hydrolysis and fermentation studies using optimized parameters through experimental design. J Agric Food Chem 58:3422–3429
Park S, Baker JO, Himmel ME, Parilla PA, Johnson DK (2010) Cellulose crystallinity index: measurement techniques and their impact on interpreting cellulose performing. Biotechnol Fuels 3:2–10
Peng F, Bian J, Peng P, Guan Y, Xu F, Sun R (2012) Fractional separation and structural features of hemicelluloses from sweet sorghum leaves. Bioresources 7:4744–4759
Peng Y, Gardner DJ, Han Y, Kiziltas A, Cai Z, Tshabalala MA (2013) Influence of drying method on the material properties of nanocellulose I: thermostability and crystallinity. Cellulose 20:2379–2392
Rao MK, Kumar A, Han SS (2017) Polysaccharide based bionanocomposite hydrogels reinforced with cellulose nanocrystals: drug release and biocompatibility analyses. Int J Biol Macromol 101:165–171
Rezzadori K, Benedetti S, Amante ER (2012) Proposals for the residues recovery: orange bagasse as raw material for products. Food Bioprod Process 9:606–614
Rivas B, Torrado A, Torre P, Converti A, Domínguez JM (2008) Submerged citric acid fermentation in orange peel autohydrolysate. J Agric Food Chem 56:2380–2387
Segal L, Creely J, Martin A, Conrad C (1962) An empirical method for estimating the degree of crystallinity of native cellulose using the X-ray diffractometer. Text Res J 29:786–794
Sudhakar DV, Maini SB (2000) Isolation and characterization of mango peel pectins. J Food Process Preserv 24:209–227
Terinte N, Ibbett R, Schuster KC (2011) Overview on native cellulose and microcrystalline cellulose I structure studied by X-day diffraction (WAXD): comparison between measurement techniques. Lenzing Ber 89:118–131
Thygesen A, Oddershede J, Lilholt H, Thomsen AB, Stahl K (2005) On the determination of crystallinity and cellulose content in plant fibres. Cellulose 12:563–576
U.S. Department of Agriculture, Foreign Agricultural Service (2017) Citrus: world markets and trade. http://www.fas.usda.gov. Accessed 8 Mar 2017
Vanderhart DL, Atalla RH (1984) Studies of microstructure in native celluloses using solid-state ^{13}C NMR. Macromolecules 17:1465–1472

Voisin H, Bergström L, Liu P, Mathew AP (2017) Nanocellulose-based materials for water purification. Nanomaterials 7:57–74

Xu X, Liu F, Jiang L, Zhu JY, Haagenson D, Wiesenborn DP (2013) Cellulose nanocrystal vs cellulose nanofibrils: a comparative on their microstructures and effects as polymer reinforcing agents. Appl Mater Interfaces 5:2999–3009

Zhao H, Kwak JH, Wang Y, Frank JA, White JM, Holladay JE (2006) Effect of crystallinity on dilute acid hydrolysis of cellulose by cellulose ball-milling study. Energy Fuel 20:807–811

Zuluaga R, Putaux JL, Cruz J, Vélez J, Mondragon I, Gañán P (2009) Cellulose microfibrils from banana rachis: effect of alkaline treatments on structural and morphological features. Carbohydr Polym 76:51–59